INTERNATIONAL JOURNAL of RENEWABLE ENERGY RESEARCH
K. Kabouchi, Vol.16, No.2, June, 2026

Computational Modeling of the Dynamic Behavior of a Proton Exchange Membrane Electrolyzer

Kaoutar Kabouchi*‡

* Equipe de modélisation des structures et systèmes mécaniques, Mohammed V University in Rabat, ENSAM, Rabat, Morocco

(kaoutar_kabouchi@um5.ac.ma)

‡Kaoutar Kabouchi, Tel: +212 00 92 77 72, kaoutar_kabouchi@um5.ac.ma

Received: 12.03.2024 Accepted: 05.05.2024

Abstract- In this study, numerical simulations were conducted to analyze the three-dimensional two-phase water/oxygen flow in the anode side flow field plate of a proton exchange membrane electrolyzer cell (PEMEC) using COMSOL Multiphysics at various times (0 s, 1 s, 2 s and 10 s). The mixture model was employed to capture the behavior of the two phases, aiming to investigate the flow characteristics within the flow field plate. Therefore, this software is used to solve numerically the complete three-dimensional model with the governing equations of continuity, momentum, and energy. The numerical findings including the velocity magnitude, the gas volume fraction distributions, and the pressure drop in the cell are presented and discussed. It is found that at 2 s and 10 s, the volume fraction of oxygen gas is highest at the plate centre of the flow field and increases from the channel entrance to the channel exit. Moreover, the flow distribution within the anode side flow field plate exhibits non-uniformity initially, particularly when gas production starts, but gradually stabilizes after reaching full oxygen production, indicating a relatively stable flow distribution between 2 s and 10 s. This work constitutes a contribution to the understanding of flow dynamics and the gas distribution within the anode side flow field plate of a PEM electrolyzer, crucial for optimizing its performance and efficiency.

Keywords PEM electrolyzer, three-dimensional model, COMSOL multiphysics, flow field plate, velocity magnitude.

1. Introduction

Renewable energy sources, such as solar, wind, and hydro, are pivotal in the transition towards sustainable energy systems due to their abundance, low environmental impact, and inexhaustible nature [1-5]. Solar power harnesses sunlight using photovoltaic cells, converting it directly into electricity [6]. Wind energy utilizes the kinetic energy of the wind to drive turbines, generating electricity [7]. Hydroelectric power taps into the gravitational force of flowing water to produce electricity through turbines [8]. These sources offer clean and renewable alternatives to fossil fuels, mitigating climate change and reducing dependency on finite resources [9]. In conjunction with renewable energy generation, Proton Exchange Membrane water electrolyzers (PEM WE) play a crucial role in energy storage and conversion [10]. PEM electrolyzers convert water into hydrogen and oxygen gases using electrical energy from renewable sources, offering a clean and efficient method for hydrogen production. This hydrogen can then be stored and used as a versatile energy carrier in various sectors, enabling the integration of renewable energy into diverse applications and facilitating the transition towards a sustainable energy future (Figure 1) [11, 12].

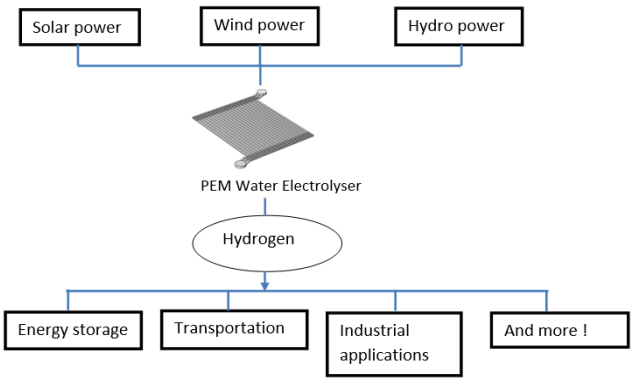

Fig. 1. Renewable energy sources and PEM electrolyzer: enabling sustainable energy systems.

Electrolysis involves the use of electricity to break down H_2O into H_2 and O_2. A PEMEC closely resembles to a Proton Exchange Membrane Fuel Cell (PEMFC). Indeed, the operation principle of PEMEC is essentially the reverse of a fuel cell. H_2O is divided into O_2, H^+, and e^- at the anode, and this reaction can be represented as:

$$H_2O \rightarrow 2e^- + 0.5O_2 \quad (1)$$

When an electric field is applied, H^+ are propelled across the PEM towards the opposite electrode (cathode), where they unite with e^- from the external circuit, resulting in the production of H_2. This process can be represented by the following reaction at the cathode:

$$2H^+ + 2e^- \rightarrow \quad (2)$$

Figure 2 illustrates the schematic of a PEMEC. It comprises the PEM, the gas diffusion layers (GDLs) on the anode and cathode sides, the water and hydrogen channels. Among these components, the bipolar plates, also known as flow field plates, are crucial as they serve as the flow distribution system basic structure [13]. These plates offer several functions, including supplying reactants to the active area of the cell, collecting current, supporting the membrane-electrode assembly (MEA) mechanically, controlling water and heat, and ensuring reactant separation [14, 15].

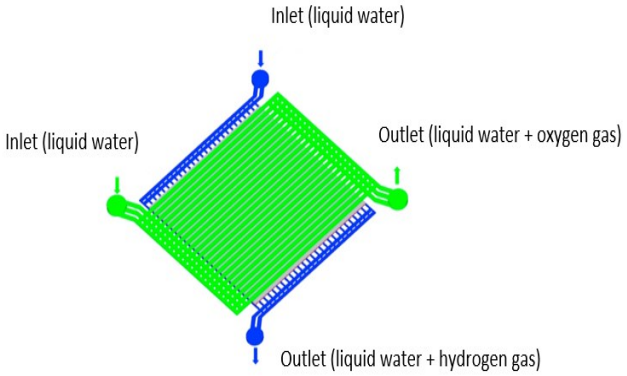

Fig. 2. PEM electrolysis cell schematic.

PEM electrolyzers are commonly used for the production of green hydrogen, which is generated through the electrolysis of water using renewable energy sources such as solar or wind power [16]. Since the study is focused on the operation of the PEMEC, the hydrogen produced is "green hydrogen". Unlike grey or blue hydrogen, green hydrogen production involves no carbon emissions and is considered environmentally friendly and sustainable.

Different methods for producing hydrogen include alkaline electrolysis [17], which utilizes an alkaline solution of potassium or sodium hydroxide as the electrolyte, offering a cheaper alternative to PEM electrolysis but with lower efficiencies and slower response times; solid oxide electrolysis [18], employing a solid ceramic material as the electrolyte to conduct negative oxygen ions from cathode to anode, achieving higher efficiencies at elevated temperatures and capable of directly electrolyzing water vapour, thereby reducing energy requirements; and photoelectrochemical (PEC) water splitting [19], utilizing sunlight on semiconducting materials to split water into H_2 and O_2 without external electrical power, although it's still largely experimental and less efficient. The computational modeling of PEMECs in the article provides various advantages including design optimization through COMSOL Multiphysics software, understanding dynamic behavior under different conditions, predictive capabilities for scaling up technology and integrating with renewable energy sources, efficiency improvement by identifying areas for enhancement such as reducing gas bubble formation, and cost reduction by enhancing operational efficiency, ultimately making hydrogen production more economically feasible.

In recent years, computational modeling has become increasingly important in understanding and optimizing the performance of electrochemical systems like PEMECs [20]. Prior research has explored various aspects of PEMECs, including electrode design, electrolyte properties, and system optimization, but often lacked the comprehensive analyzis of flow dynamics and gas distribution over various time intervals. Indeed, the dynamic behavior within the flow field plate, especially regarding flow distribution phenomena, remains a delicate and critical aspect.

The present research focuses on using computational modeling, particularly using COMSOL Multiphysics, to analyze the dynamic behavior of PEMEC, specifically within the anode side flow field plate. It addresses the intricate flow distribution phenomena within the plate, crucial for optimizing operational efficiency.

Numerous researchers have dedicated efforts to enhance flow uniformity within flow field plates, primarily focusing on fuel cells in their published findings. Upadhyay et al. [21] employed numerical methods to investigate how various operational parameters affect the PEMEC performance. They discovered that low GDL porosity, high cathode pressure, and low water input rate increase the power required to run the electrolyzer effectively using the ANSYS Fluent solver. Lee et al. [22] introduced a 2D computational fluid dynamics (CFD) model to analyze gas distribution across the cathode and gas diffusion layer (CL-GDL) interface. Their findings suggested that optimizing operating temperatures enhances O_2 and H_2O transport within the GDL. A computational fluid dynamics investigation by Xu et al. [23] examined the anode flow field of the PEMWE while taking two-phase flow effects into account. According to their findings, a parallel flow distributor is less successful than a serpentine flow distributor at eliminating oxygen gas bubbles. A three-dimensional model was developed by Olesen et al. [24] for high-pressure PEMECs to assess the suitability of circular and interdigitated anode flow field designs under high current densities.

In this study, the Electrochemistry Module of the COMSOL Multiphysics software is used to develop a 3D mathematical model that simulates the behavior of the anode side flow field plate of a PEMEC at different times 0 s, 1 s, 2 s, and 10 s under various parameters, such as the velocity magnitude, the gas volume fraction distributions, and the pressure drop in the cell. In fact, the study focuses on the dynamic behavior within the anode side flow field plate of PEMEC, which is a key component in the production of H_2 through water electrolysis, and the oxygen gas produced in the anode side which is accompanied by the generation of H_2 gas at the cathode side. The computational model allows for a detailed understanding of the flow dynamics and the gas dispersion within the PEMEC, which directly relates to

hydrogen production. In addition, the flow dynamics and the gas distribution directly contribute to the efficient generation of hydrogen related to the electrolysis process.

2. Mathematical Modeling

2.1. Geometric Model

Fig. 3 shows a three-dimensional model of the anode side flow field plate of a PEMEC. It features one cylindrical inlet port and one exit port, both positioned diagonally. The circular inlet at the upper boundary of the cylinder distributes liquid water into a manifold. The manifold then evenly distributes the flow across 23 channels. Below these channels, the anode electrode generates oxygen gas. The resulting two-phase mixture of liquid water and oxygen gas exits the cell through the exit manifold. Based on the parameters in Table 1, geometrical model was developed in COMSOL Multiphysics software for simulation and visualization of its flow pattern.

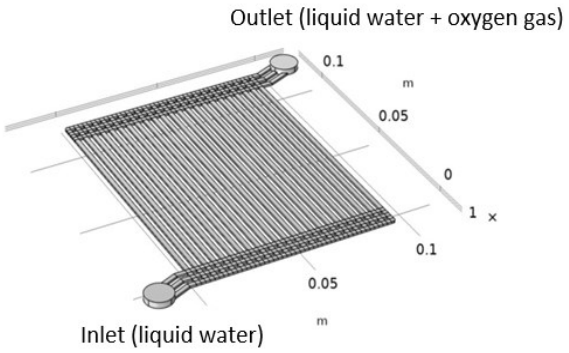

Fig. 3. Model geometry.

Table 1. Design parameters

Description	Value
Number of electrodes channels, full cell N_ch_full_cell	23
Electrode channel lengths L_ch (m)	0.1049
Rotation angle, inlet/outlet ang_inout (rad)	0.3927
Channel height h_a (m)	8.89e-4
Inlet/outlet channel length L_inout (m)	0.02
Radius of inlet tube R_in (m)	0.00635
Channel width w_ch (m)	0.00207
Oxygen bubble diameter D_bubbles (m)	1e-5

2.2. Basic Assumptions

An isothermal system, laminar flow, incompressible fluid, constant thermo-physical characteristics, a three-dimensional, stable model, ideal gases for all gases, and isotropic materials are among the assumptions.

2.3. Governing Equations

The mathematical expressions for continuity, momentum, and energy can be outlined as follows [25]:

Continuity equation:

$$\nabla.(\rho\vec{U}) = 0 \quad (4)$$

where ρ (kg/m3) is the fluid density and is the velocity vector of the fluid.

Momentum equation:

$$\rho(\vec{U}.\nabla)\vec{U} = -\nabla p + \mu\Delta\vec{U} \quad (5)$$

where μ (kg/m.s) indicates the viscosity and p indicates the pressure (Pa).

Energie equation:

$$\nabla.(\rho\vec{U}C_p T) = k(\Delta T) \quad (6)$$

where C_p is the specific heat capacity, T (K) is the temperature and k (W/m.K) is the thermal conductivity.

2.4. Basic Assumptions

The setup of the model involves utilizing the Mixture Model and Laminar Flow interface, where the continuous phase is defined by liquid water, and the dispersed phase is represented by oxygen gas bubbles. The assumptions made include incompressible and isothermal conditions.
The liquid water is entering at a flow rate of 260 ml/min, which is specified through an Inlet boundary condition.
At the interfaces between the electrode surface and the channel, liquid water is utilized, leading to the generation of oxygen gas in accordance with:

$$2H_2O(l) \rightarrow O_2(g) + 4H^+ + 4e^- \quad (7)$$

The polymer membrane facilitates the movement of protons, separating the two electrode compartments and directing them to the cathode side of the electrolyzer cell. Alongside the generation of oxygen gas, there is a resulting net mass outflow attributable to proton transport at the boundaries of the electrode surface and channels.
The total oxygen production rate of 5 mg/s is established by utilizing an Inlet boundary condition node, which combines the production of oxygen gas with the overall mass outflow.
At the outlet boundaries, a pressure condition is applied, while for all other boundaries, a no-slip wall condition is specified.

3. Numerical Procedure

In simulations using CFD, the structure of the mesh plays a crucial role in achieving accurate results within a short computational time. The schematic configuration of the COMSOL Multiphysics software's computational domain for the anode side flow field plate of the PEMEC with 23 channels is shown in Figure 4. This study utilized two types of elements: tetrahedral elements in the inlet and outlet manifolds of the bipolar plate and hex elements in the central channels of the flow field plate.

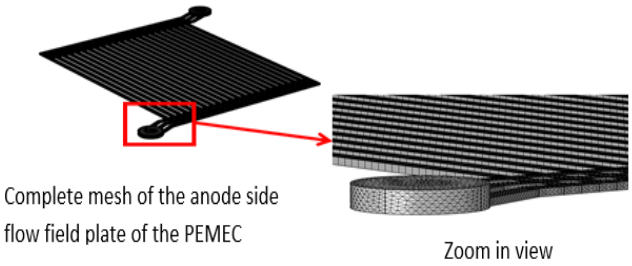

Fig. 4. Structure meshing.

4. Results and Discussions

Numerical simulations were conducted using COMSOL Multiphysics for the three-dimensional model of the anode side flow field plate of a PEMEC at different times (0 s, 1 s, 2 s and 10 s) and the results are discussed. Key parameters, such as velocity magnitude, gas volume fraction and pressure drop in the cell, are illustrated in Figures 5-8.

4.1. Velocity Magnitude

Figure 5 depicts the mass-averaged velocity magnitude distribution at various times. It is observed that as we move from t = 0 s to t = 10 s, the velocity magnitude increases. The manifold channels at the inlet and outlet have the highest velocities. At t=0s (Figure 5 (a)), meanwhile, the velocity magnitude distribution shows a relatively uniform flow pattern throughout the system, with no significant variations in velocity along the manifold channels. Subsequently, at t=1s (Figure 5 (b)), slight increases in velocity magnitude are noticeable along the manifold channels, indicating the initiation of flow acceleration within the system. As time progresses, at t=2s (Figure 5 (c)), the velocity magnitude continues to rise, with more pronounced velocity gradients along the manifold channels, suggesting further acceleration of the flow. Finally, at t=10s (Figure 5 (d)), the velocity magnitude distribution exhibits the highest values along the manifold channels at the inlet and outlet, indicating the culmination of flow acceleration processes within the system.

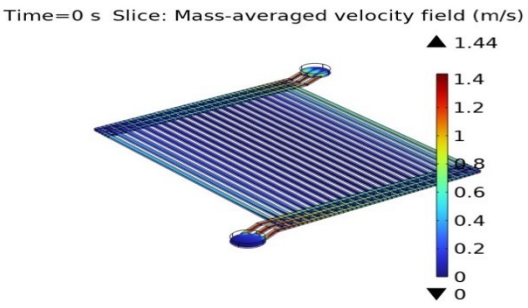

(a)

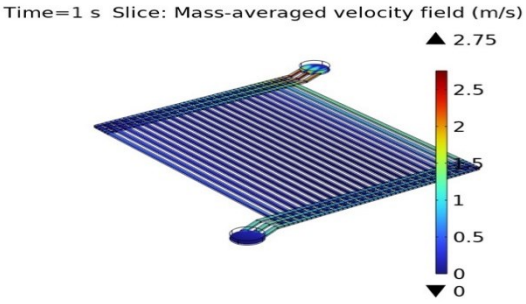

(b)

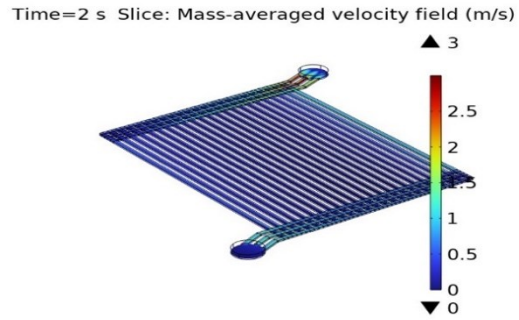

(c)

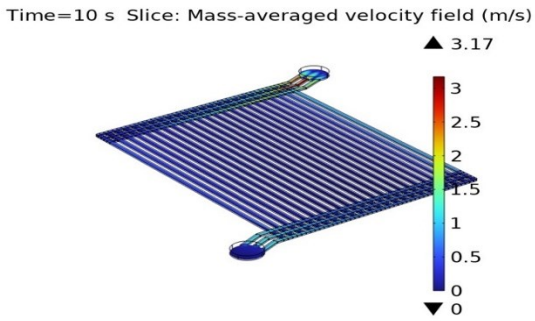

(d)

Fig. 5. Velocity magnitude distribution at (a) 0 s, (b) 1 s, (c) 2 s and (d) 10 s.

4.2. Volume Fraction of Gas in the Cell

In Figure 6, the distribution of gas volume fraction resulting from oxygen evolution within the cell is depicted at various times. This figure shows that the gas volume fraction in the cell increases as the time ranges from 0 s to 10 s. By 2 s and 10 s, the gas volume fraction reaches nearly 100% towards the terminus of the electrode flow channels situated within the central region of the flow field. At t=0s (Figure 6 (a)), the gas volume fraction within the cell is minimal. Consequently, it is predominantly confined to the electrode-electrolyte interface due to the initial stages of oxygen evolution. Subsequently, at t=1s (Figure 6 (b)), the gas volume fraction begins to propagate outward from the electrode-electrolyte interface. As a result, there is a slight increase in volume fraction within the flow channels. Then, at t=2s (Figure 6 (c)), the gas volume fraction further expands within the flow channels. This indicates the progression of oxygen evolution and the filling of the channels with gas. Finally, at t=10s (Figure 6 (d)), the gas volume fraction approaches saturation within the flow

channels. Consequently, it is nearing 100%, indicating a nearly complete conversion of H_2O to O_2 gas at the electrode surfaces. This observation aligns with the results documented in reference [26], where Özdemir and Taymaz conducted a comprehensive three-dimensional modeling of gas-liquid flow in the anode bipolar plate of a PEM electrolyzer. Their findings corroborate the gradual increase in gas volume fraction over time, indicating the progression of oxygen evolution within the flow channels. Additionally, they highlight the significance of the electrode-electrolyte interface in facilitating gas generation and its subsequent propagation within the cell.

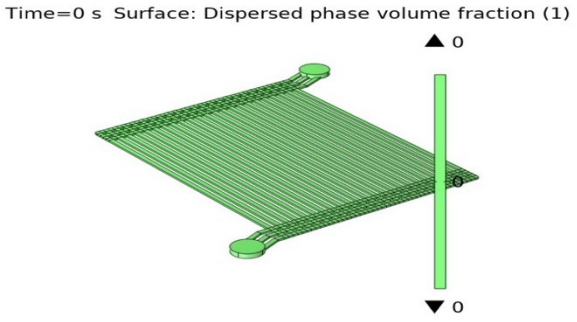

(a)

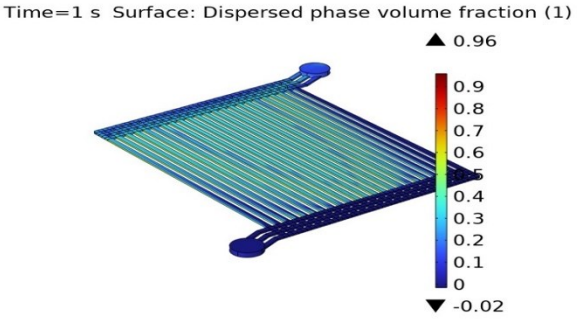

(b)

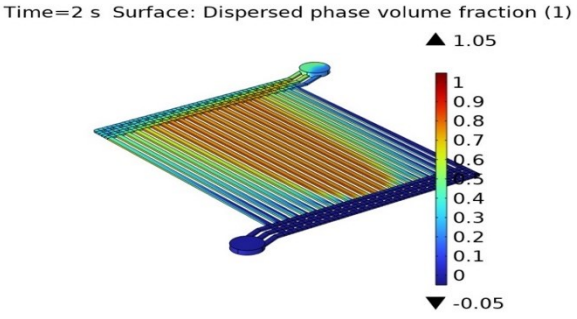

(c)

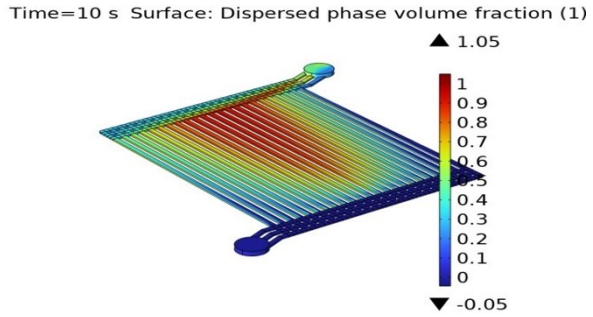

(d)

Fig. 6. Volume fraction of gas in the cell at (a) 0 s, (b) 1 s, (c) 2 s and (d) 10 s.

4.3. Pressure Distribution

Figure 7 illustrates the variation in pressure drop within the anode flow field at various times. It is observed that the pressure drop across the entire flow field experiences a minor increase due to the evolution of oxygen gas. At t=0s (Figure 7 (a)), the pressure drop remains relatively stable as the electrolyzer begins operation, with minimal gas evolution and flow disturbances. However, at t=1s (Figure 7 (b)), there is a slight uptick in pressure drop as the generation of oxygen gas initiates within the anode flow field, leading to a slight obstruction in flow paths. Subsequently, at t=2s (Figure 7 (c)), the pressure drop continues to increase marginally as the production of oxygen gas progresses, resulting in a gradual build-up of pressure within the flow field. For t=10s (Figure 7 (d)), the pressure drop reaches a relatively steady state, with the evolution of O_2 gas stabilizing and the flow field adapting to the altered conditions, resulting in a minor but sustained increase in pressure drop across the system. This result is consistent with the findings of Nie and Chen [27] which utilized numerical modeling to investigate the behavior of two-phase gas-liquid flow in the flow field plate of a PEM electrolysis cell, highlighting similar trends in pressure drop variation.

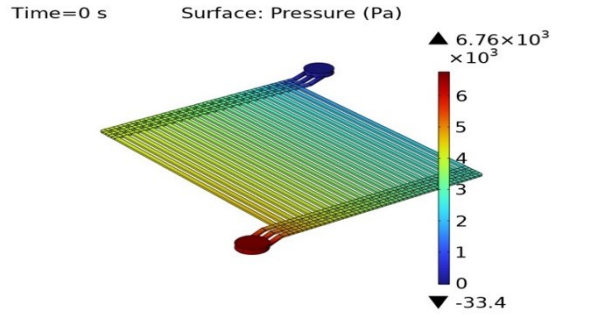

(a)

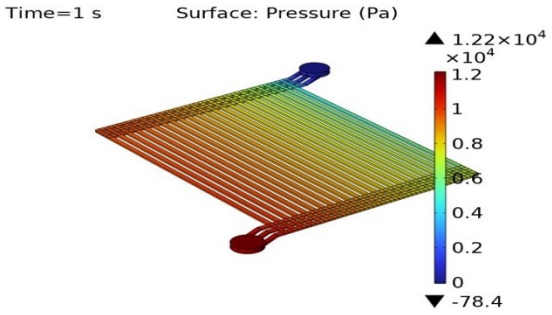

(b)

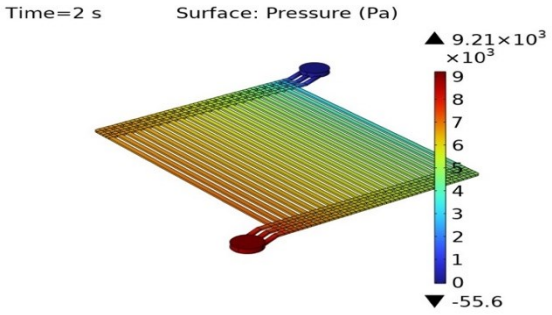

(c)

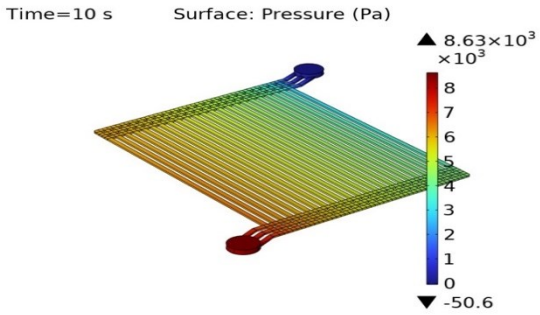

(d)

Fig. 7. Pressure drop in the cell at (a) 0 s, (b) 1 s, (c) 2 s and (d) 10 s.

4.4. Velocity in Electrode Channels at Various Times

In Figure 8, the velocity magnitudes are depicted at half the length in the y-direction and half in the height in the z-direction of the electrode channels at various times. This representation holds significance as it provides insights into the uniformity of flow distribution across individual channels. The plot reveals that the flow distribution is not particularly uniform during the initial stage with pure water (0 s). However, it becomes notably less uniform when gas production commences (1 s and 2 s). For 10 s, the distribution relaxes to a somewhat more uniform profile, but still less uniform than that observed with pure water. Additionally, it is evident that the flow field distribution remains relatively stable between 2 s and 10 s. This observation suggests the establishment of a stationary flow distribution shortly after achieving full oxygen production at 1 s.

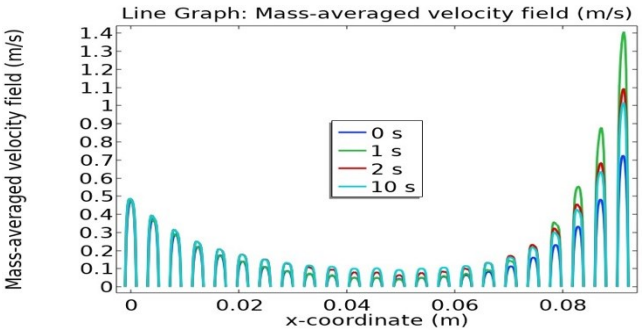

Fig. 8. Individual channel velocities at various times.

5. Conclusion

The main contribution of the article is the development of a comprehensive numerical model using COMSOL Multiphysics to simulate the dynamic behavior within the anode side flow field plate of a PEMEC. This model allows for the investigation of flow characteristics in the flow field plate over different time intervals (0 s, 1 s, 2 s, and 10 s). The significance of this work lies in the ability to enhance our understanding of the flow dynamics and the gas dispersion within the PEMEC, which is crucial for improving its operational efficiency. By analyzing parameters such as velocity magnitude, gas volume fraction distribution, and pressure drop, the study provides insights into the non-uniform flow distribution during gas production onset and its stabilization once full oxygen production is achieved. This understanding can inform the design and operation of PEMECs, thereby facilitating the development of more efficient hydrogen production systems for various applications, including renewable energy storage and fuel cell technology. The novelties of this research include the utilization of a mixture model based on COMSOL Multiphysics to investigate the gas-liquid flow in the anode side flow field plate of a PEMEC. Additionally, the study highlights the non-homogeneous distribution of velocity and oxygen gas volume fraction within the flow field plate, as well as the stabilization of flow distribution over time. Possible applications and extensions of this work could involve further optimizing the design of PEMECs based on the insights gained from the numerical modeling study. This could include refining the flow field plate geometry to improve flow distribution and efficiency, as well as exploring different operating conditions to enhance overall performance. Additionally, the numerical model developed in this study could be adapted and applied to investigate other aspects of PEMECs or similar electrochemical systems, potentially advancing research in the field of renewable energy production and storage.

Acknowledgements

This work is supported by Mohammed V University in Rabat. The author gratefully acknowledges the support.

Author Contributions

Kaoutar Kabouchi was responsible for the conceptualization of the study, methodology, numerical modeling, simulations, data analysis, and manuscript writing. The author has read and agreed to the published version of the manuscript.

Conflict of Interest

The author(s) declare(s) that there is no conflict of interest regarding the publication of this article.

References

[1] W. M. Fendzi, S. R. N. Dzonde, R. J. J. Molu, and S. K. Tsobze, "Contribution into robust optimization of renewable energy sources: Case study of a standalone hybrid renewable system in Cameroon," International Journal of Renewable Energy Research, vol. 13, no. 3, pp. 1093–1120, 2023.

[2] A. G. Abdullah, D. L. Hakim, N. T. Sugito, and D. Zakaria, "Investigating evolutionary trends of hybrid renewable energy systems: A bibliometric analysis from 2004 to 2021," International Journal of Renewable Energy Research, vol. 13, no. 1, pp. 376–391, 2023.

[3] H. Messaoudi, A. B. Abdelghani-Bennani, N. M. Bellaaj, and M. Orabi, "Genetic algorithm-based thermal parameters identification for renewable energy system converters," International Journal of Renewable Energy Research, vol. 12, no. 3, pp. 1692–1703, 2022.

[4] M. J. B. Kabeyi and O. A. Olanrewaju, "Sustainable energy transition for renewable and low carbon grid electricity generation and supply," Frontiers in Energy Research, vol. 9, p. 1032, 2022.

[5] W. Strielkowski, L. Civín, E. Tarkhanova, M. Tvaronavičienė, and Y. Petrenko, "Renewable energy in the sustainable development of electrical power sector: A review," Energies, vol. 14, no. 24, p. 8240, 2021.

[6] M. M. Hasan, S. Hossain, M. Mofijur, Z. Kabir, I. A. Badruddin, T. M. Yunus Khan, and E. Jassim, "Harnessing solar power: A review of photovoltaic innovations, solar thermal systems, and the dawn of energy storage solutions," Energies, vol. 16, no. 18, p. 6456, 2023.

[7] M. Z. Hossain, S. A. Rahman, M. I. Hasan, M. R. Ullah, and I. M. Siddique, "Evaluating the effectiveness of a portable wind generator that produces electricity using wind flow from moving vehicles," Journal of Industrial Mechanics, vol. 8, no. 2, pp. 44–53, 2023.

[8] M. Z. Almuzakki, "Mathematical modelling in energy measurement production of water tap flow," Journal of Science and Informatics for Society, vol. 1, no. 1, 2023.

[9] P. A. Owusu and S. Asumadu-Sarkodie, "A review of renewable energy sources, sustainability issues and climate change mitigation," Cogent Engineering, vol. 3, no. 1, p. 1167990, 2016.

[10] Z. Chen, L. Guo, L. Pan, T. Yan, Z. He, Y. Li, and J. J. Zou, "Advances in oxygen evolution electrocatalysts for proton exchange membrane water electrolyzers," Advanced Energy Materials, vol. 12, no. 14, p. 2103670, 2022.

[11] S. Singh, S. Jain, P. S. Venkateswaran, A. K. Tiwari, M. R. Nouni, J. K. Pandey, and S. Goel, "Hydrogen: A sustainable fuel for future of the transport sector," Renewable and Sustainable Energy Reviews, vol. 51, pp. 623–633, 2015.

[12] L. Zhang, C. Jia, F. Bai, W. Wang, S. An, K. Zhao, and H. Sun, "A comprehensive review of the promising clean energy carrier: Hydrogen production, transportation, storage, and utilization (HPTSU) technologies," Fuel, vol. 355, p. 129455, 2024.

[13] H. Kahraman and M. F. Orhan, "Flow field bipolar plates in a proton exchange membrane fuel cell: Analysis and modeling," Energy Conversion and Management, vol. 133, pp. 363–384, 2017.

[14] E. H. Majlan, D. Rohendi, W. R. W. Daud, T. Husaini, and M. A. Haque, "Electrode for proton exchange membrane fuel cells: A review," Renewable and Sustainable Energy Reviews, vol. 89, pp. 117–134, 2018.

[15] X. Z. Yuan, C. Nayoze-Coynel, N. Shaigan, D. Fisher, N. Zhao, N. Zamel, and U. Groos, "A review of functions, attributes, properties and measurements for the quality control of proton exchange membrane fuel cell components," Journal of Power Sources, vol. 491, p. 229540, 2021.

[16] N. S. Hassan, A. A. Jalil, S. Rajendran, N. F. Khusnun, M. B. Bahari, A. Johari, and M. Ismail, "Recent review and evaluation of green hydrogen production via water electrolysis for a sustainable and clean energy society," International Journal of Hydrogen Energy, vol. 52, part B, pp. 420–441, 2024.

[17] C. Li and J. B. Baek, "The promise of hydrogen production from alkaline anion exchange membrane electrolyzers," Nano Energy, vol. 87, p. 106162, 2021.

[18] X. Zhang, B. Liu, Y. Yang, J. Li, J. Li, Y. Zhao, and Y. Sun, "Advances in component and operation optimization of solid oxide electrolysis cell," Chinese Chemical Letters, vol. 34, no. 5, p. 108035, 2023.

[19] C. Jiang, S. J. Moniz, A. Wang, T. Zhang, and J. Tang, "Photoelectrochemical devices for solar water splitting-materials and challenges," Chemical Society Reviews, vol. 46, no. 15, pp. 4645–4660, 2017.

[20] B. Han, J. Mo, Z. Kang, G. Yang, W. Barnhill, and F. Y. Zhang, "Modeling of two-phase transport in proton exchange membrane electrolyzer cells for hydrogen energy," International Journal of Hydrogen Energy, vol. 42, no. 7, pp. 4478–4489, 2017.

[21] M. Upadhyay, A. Kim, S. S. Paramanantham, H. Kim, D. Lim, S. Lee, and H. Lim, "Three-dimensional CFD simulation of proton exchange membrane water electrolyser: Performance assessment under different condition," Applied Energy, vol. 306, p. 118016, 2022.

[22] C. H. Lee, J. K. Lee, B. Zhao, K. F. Fahy, J. M. LaManna, E. Baltic, and A. Bazylak, "Temperature-dependent gas accumulation in polymer electrolyte membrane electrolyzer porous transport layers," Journal of Power Sources, vol. 446, p. 227312, 2020.

[23] Y. Xu, G. Zhang, L. Wu, Z. Bao, B. Zu, and K. Jiao, "A 3-D multiphase model of proton exchange membrane electrolyzer based on open-source CFD," Digital Chemical Engineering, vol. 1, p. 100004, 2021.

[24] A. C. Olesen, S. H. Frensch, and S. K. Kær, "Towards uniformly distributed heat, mass and charge: A flow field design study for high pressure and high current density operation of PEM electrolysis cells," Electrochimica Acta, vol. 293, pp. 476–495, 2019.

[25] M. Manninen, V. Taivassalo, and S. Kallio, "On the mixture model for multiphase flow."

[26] S. N. Özdemir and I. Taymaz, "Three-dimensional modeling of gas-liquid flow in the anode bipolar plate of a PEM electrolyzer," Journal of the Brazilian Society of Mechanical Sciences and Engineering, vol. 44, no. 8, p. 354, 2022.

[27] J. Nie and Y. Chen, "Numerical modeling of three-dimensional two-phase gas-liquid flow in the flow field plate of a PEM electrolysis cell," International Journal of Hydrogen Energy, vol. 35, no. 8, pp. 3183–3197, 2010.